

## Optimal design of the switched reluctance motor to the electric vehicle

**Abstract.** The paper presents the algorithm and procedure for optimization of the switched reluctance motor. The switched reluctance motor (SRM) with an 8/6 structure is optimized. Two design variables are taken into account in the optimization process. Such types of SRM are commonly used in hybrid electric vehicles and aerospace applications. The main aim of our work is to increase the performance parameters of electric vehicles and to make them more optimized for low cost by using suitable dimensions of motor and different kind of design materials. In the objective functions the electromagnetic torque, the torque ripple, and the mass of the core are taken into consideration. The optimization calculation is executed in the 2D finite element method. The performance characteristics are determined for both optimal structures. Selected results of the calculation are presented and discussed.

**Streszczenie.** W artykule przedstawiono algorytm i oprogramowanie do optymalizacji silnika reluktancyjnego o konfiguracji 8/6. W procesie optymalizacji uwzględnione zostały dwie zmienne projektowe opisujące strukturę silnika. Do optymalizacji zastosowano metodę salpów, zaś ograniczenia uwzględniono przy wykorzystaniu metody funkcji kary zewnętrznej. Celem procedury optymalizacyjnej jest poprawa parametrów funkcjonalnych silnika przeznaczonego do napędu rikszy rowerowej. W kompromisowej funkcji celu uwzględniono: moment elektromagnetyczny, tętnienia momentu oraz masę rdzenia. Wykonano obliczenia optymalizacyjne dla dwóch różnych materiałów z którego wykonano rdzeń. Przedstawiono i omówiono wybrane wyniki obliczeń optymalizacyjnych (**Optymalna konstrukcja przełączanego silnika reluktancyjnego do pojazdu elektrycznego**).

**Keywords:** constrained optimization, salp swarm algorithm, switched reluctance motor, finite element analysis

**Słowa kluczowe:** optymalizacji z ograniczeniami, metoda salpów, silnik synchroniczny reluktancyjny

### Introduction

Switched reluctance motor (SRM) operates using magnetic reluctance changes in the magnetic circuit. Such types of motors are economical due to height efficiency and low maintenance costs. The main disadvantages of SRM are height torque ripples, vibration, and acoustic noise. During optimal design the reduction of torque ripple is necessary. The application of different types of material had an impact on the noise level [1].

Industries using the switched reluctance motor with a high no of rotor poles are discussed [2]. The torque improvement of SRM is employed and the corresponding results are given. In third generation hybrid electric vehicles are used in industries with SRM are designed [3]. In [4] comparing rare earth PM motor with SRM. In [5] vibration reduction and pole section of SRM is explained. In [6] design of a hybrid electric vehicle for less rare earth magnets is discussed. In [7] design of hybrid electric vehicles and a comparison of PM drive motors with cage induction motors are given. In [8] wheel SRMs are often designed by the use of multi-objective optimization. In [9,, 10] designation of SRM of pole section and vibration reduction of motor and also rare earth magnet with high power density excited in hybrid mode is discussed. The ratio of external rotor diameter to length of stack length in the outer rotor type of SRM is influenced. SRM with the optimal ratio is used to improve the torque [8, 11].

The salp swarm algorithm (SSA) belongs to the swarm intelligence optimization method. The last research show, that this method is much better convergent than the particle swarm optimization and ant colony optimization methods [12].

The optimization calculations were performed for the 8/6 switched reluctance motor configuration with four phases.. The best performance was achieved with an optimal ratio of the external periphery of the rotor to the axial length ( $D/L$ ). Additionally, increasing the pole counts also improved performance. Although these types of vehicles are commonly found in the market, our main goal in selecting

parameters is to increase the efficiency and performance of electric vehicles while keeping costs low. This can be achieved by using suitable dimensions of the motor and different types of design materials.

### Equations switched reluctance motor structure

The investigated switched reluctance motor has 8 poles in the stator and 6 poles in the rotor. The winding is made from 8 concentrated coils connected in pairs. The structure of the magnetic circuit is presented in Figure 1.

The main structure parameters of the motor are presented in Table 1. The optimized motor was described by two design variables: (a) outer stator diameter to stack length ratio, and (b) stator and rotor pole arc.

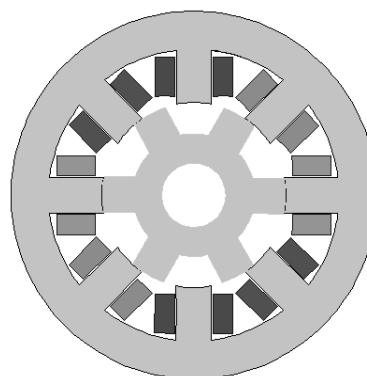


Fig.1. Structure of the 8/6 4 phase SRM structure

### Salp swarm algorithm

The salp swarm algorithm was proposed by Mirjalili in 2017 [13]. This optimization algorithm belongs to the swarm intelligence method group. Recent research has shown that it is more effective than the classical particle swarm algorithm. The SSA was elaborated on observations of the social behavior of the salps colony during foraging. The slaps move by creating long string colonies, called chains.

Slaps are barrel-shaped ocean animals. They move shrinking bands of muscles and pumping water by their own body.

Table 1. Structural parameters of the SRM

Parameter	Data	
	Unit	Value
Number of stator poles	[-]	8
Number of rotor poles	[-]	6
Stator outer diameter	[mm]	128
Inner stator diameter	[mm]	100
Air gap length	[mm]	0.36
Diameter of the stator poles	[mm]	63.35
Rotor slot bottom diameter	[mm]	42
Shaft diameter	[mm]	22
Number of turns in single coil	[-]	126
Number of phases	[-]	4
Nominal mechanical power	[W]	750
Supply voltage (DC)	[V]	48

The mathematical description of the salps' behavior and creating chain is divided the salp population (salp swarm) into two separate groups: leader (leaders) and followers. The leader (best-adapted individual) should be located at the front of the chain. The leaders' group can be created by a few salps [14]. In such an approach, the everyone member of the leader group follows after the previous individual.

The salp swarm system is defined in the  $d$ -th dimensional permissible area, where  $d$  denotes the number of design variables. The slap swarm system is described by the following matrix:

$$(1) \quad \mathbf{X} = \begin{bmatrix} x_1^1 & x_2^1 & \dots & x_d^1 \\ x_1^2 & x_2^2 & \dots & x_d^2 \\ \vdots & \vdots & \ddots & \vdots \\ x_1^N & x_2^N & \dots & x_d^N \end{bmatrix}$$

where  $N$  is the number of slaps.

The position of a single  $i$ -th salp is described by a vector:

$$(2) \quad x^i = [x_1^i, x_2^i, \dots, x_d^i]^T$$

The first operation of the salp swarm algorithm is the generation of the initial population. The initial population is usually created randomly. Next, the evaluation of all salps in the population is made taking into account the fitness function (objective function). It is assumed, that the salp colony goal is the food source ( $\mathbf{F}_s$ ) [15].

The leader position (the best-adapted individual in the population) is calculated by the equation:

$$(3) \quad \mathbf{x}^l = \begin{cases} \mathbf{F}_s + a_1[a_2(\mathbf{x}_{\max} - \mathbf{x}_{\min}) + \mathbf{x}_{\min}] & \text{for } a_3 \geq 0 \\ \mathbf{F}_s - a_1[a_2(\mathbf{x}_{\max} - \mathbf{x}_{\min}) + \mathbf{x}_{\min}] & \text{for } a_3 < 0 \end{cases}$$

where:  $\mathbf{x}^l$  is the position of the leader,  $a_1, a_2$ , are the random number from range (0, 1),  $\mathbf{x}_{\min}$  and  $\mathbf{x}_{\max}$  are the vectors of the lower and upper range of design variables.

The salp swarm characteristic coefficient  $a_1$  value is changed during the optimization process. In  $k$ -th iteration,  $a_1$  coefficient is determined as:

$$(4) \quad a_1 = 2e^{-\left(\frac{2k}{k_{\max}}\right)}$$

where  $k_{\max}$  is the maximum number of iterations.

The the  $k$ -th iteration the position the  $i$ -th follower is determined:

$$(5) \quad \mathbf{x}_k^i = \frac{1}{2}(\mathbf{x}_k^i - \mathbf{x}_{k-1}^i)$$

### The sizing optimization of the switched reluctance motor

The SRM is defined by two design variables: (a)  $x_1=D/L$ , and (b)  $x_2=\alpha$ , where  $L$  is the stack length of the motor,  $D$  is the outer diameter of the stator,  $\alpha$  is the stator and rotor angle span. The ranges of design parameters are presented in Table 2. The rest structural parameters of the optimized SRM are constant (see Table 1) during the optimization process.

Table 2. The upper and lower values of the design variables

Design variable	Lower	Upper
$x_1$	0.4	2.7
$x_2$	18	23

The mathematical model of 4-phase SRM was developed by using RMxpert. Next, the 2-D finite element method model was created. The elaborated model allows to calculate: (a) the average value of electromagnetic torque, (b) torque ripple, (c) efficiency, and (d) the total mass of SRM cores (stator and rotor).

The optimum design of SRM usually focuses on the maximization of the average electromagnetic torque and the minimization of torque ripple [16]. Also, efficiency and total mass are taken into account as optimality criteria [17]. Torque ripple is calculated using the method described in [18].

In the elaborated optimization procedure three functional parameters included into the multi-objective optimization function. The objective function for the  $i$ -th salp is calculated:

$$(6) \quad f^i(x_1, x_2) = \lambda_1 \left( \frac{T_{av}^i(x_1, x_2)}{T_{av_0}^i} \right) + \lambda_2 \left( \frac{T_{r_{av}}}{T_{r_{av}}^i(x_1, x_2)} \right) + \lambda_3 \left( \frac{m_{av}}{m^i(x_1, x_2)} \right)$$

where:  $T_{av}(x_1, x_2)$ ,  $T_r(x_1, x_2)$ ,  $m(x_1, x_2)$  are the average electromagnetic torque, torque ripple, and total mass of the motor,  $T_{av_0}$ ,  $T_{r_{av}}$ , and  $m_{av}$  are the values of these parameters calculated as an average value of such parameters for an initial swarm,  $\lambda_1, \lambda_2, \lambda_3$  are the weighting coefficients.

The optimization procedure maximizes the primary objective function  $f(x_1, x_2)$ , while the non-linear constraint has been taken into consideration. The non-linear constraint concerns the efficiency of the designed machine. The imposed efficiency  $\eta(x_1, x_2) \geq \eta_z$ , where  $\eta_z$  is the imposed value of efficiency. The normalized constraint was been calculated as follows:

$$(7) \quad g^i(x_1, x_2) = \frac{\eta_z - \eta^i(x_1, x_2)}{\eta_z}$$

The imposed efficiency was taken into account by the external penalty function [19]. In the external penalty approach, the penalty term determining the overstepping from the imposed efficiency is calculated as:

$$(8) \quad p^i(x_1, x_2) = \sigma^n g^i(x_1, x_2)$$

where  $\sigma$  is the penalty coefficient,  $n$  is the external penalty iteration.

In the constrained optimization tasks, the external penalty iteration ( $n$ ) is usually interlaced with the iteration of the salp swarm algorithm ( $k$ ) [20, 21]. The value of the penalty coefficient is updated (increased) after executing a given number of iterations of the salp algorithm. The

optimization procedure is finished after executing the maximum number of external penalty iterations ( $n_{max}$ ).

In constrained optimization, the modified objective function  $h(\mathbf{x})$ , composed from: (a) primary objective function and (b) penalty term is taken into consideration.

$$(9) \quad h^i(\mathbf{x}) = \begin{cases} f^i(x_1, x_2) & \text{for } \eta(\mathbf{x}) \geq \eta_z \\ f^i(x_1, x_2) - p^i(x_1, x_2) & \text{for } \eta(\mathbf{x}) < \eta_z \end{cases}$$

where  $\mathbf{x} = (x_1, x_2)$  is the vector of design variables.

The optimization calculations have been performed on two materials used for the production of stator and rotor core, such as M-19 and steel 1010. The M-19 laminated silicon steel material is the most important grade material used for motion-controlling electrical machines, as it has the lowest core losses in this type of material. The steel 1010 has lower strength relatively but due to quenching and tempering strength increases. For steel 1010, the machinability in the states of cold drawn and cold worked is fairly good. This material consists of good formability and ductility properties and is also easily welded.

Optimization calculations were made for the number of salps equal to 40 and the number of iterations 24. In a single external iteration related to the increase of the penalty term, six iterations of the slap algorithm were executed. The weighting coefficient in primary objective function was assumed:  $\lambda_1=0.4$ ,  $\lambda_2=0.35$ ,  $\lambda_3=0.25$ . The penalty coefficient was adopted  $\sigma=1.2$ . The  $\lambda_1$ ,  $\lambda_2$  and  $\lambda_3$  coefficients were determined on the basis of the first three iterations of the optimization algorithm for random positions of the salps [21]. The weighting factors were selected to obtained output torque bigger than 2.25 Nm, torque ripple smaller than 33 % and mass smaller than 4.4 kg.

The imposed value of  $\eta_z=83$  % was assumed. The optimization process was repeated for different initial populations.

The course of the optimization process for selected iterations ( $k$ ) is presented in Table 3. The following columns represent the values of decision variables, electromagnetic torque, torque pulsations, material mass, efficiency, and modified objective function. Only the results for the slap leader are taken into account.

Table 3. The course of the optimization process for M-19 material

$k$	$x_1$	$x_2$	$T_{av}$	$T_r$	$m$	$\eta$	$h$
[-]	[-]	[°]	[Nm]	[%]	[kg]	[%]	[-]
1	1.77	22	2.69	34.85	6.12	86.5	0.951131
3	1.53	21	3.98	43.19	7.76	70.38	1.127168
5	2.5	20	1.73	35.39	4.39	83.20	1.352387
10	2.22	21	2.86	32.55	3.86	82.96	1.468821
24	2.22	21	2.86	32.55	3.86	82.96	1.468821

Next the optimization calculations were performed for the steel 1010. The results for selected iterations of salp swarm algorithm were presented in Table 4.

Table 4. The course of the optimization process for steel 1000 material

$k$	$x_1$	$x_2$	$T_{av}$	$T_r$	$m$	$\eta$	$h$
[-]	[-]	[°]	[Nm]	[%]	[kg]	[%]	[-]
1	2.0	22	3.91	4.68	13.52	93.08	0.909549
3	1.25	21	5.01	36.65	11.89	89.20	1.164222
5	1.538	21	2.90	43.24	2.84	72.31	1.220196
10	2.50	21	2.27	36.33	4.28	86.50	1.569931
24	2.50	21	2.27	36.33	4.28	86.50	1.569931

The optimization of SRM machines was executed. The stator and rotor core of both machines are made from materials with different properties. As a result of the

optimization processes, the same values of the  $x_2$  variable were obtained for both analyzed materials, while the values of the  $x_1$  variable differed. The SRM made of the M-19 material is characterized by a higher value of the average torque and lower values of the torque ripple and the core mass concerning the SRM made of steel 1010 material. The steel core SRM has a higher efficiency value. The rated speed for the SRM motor with the core made from M-19 steel was 2495.2 rpm. Whereas the rated velocity for optimal motor produced from steel 1010 was 2420 rpm.

Next, the performances characteristic of optimal SRM machines are determined. The characteristic is determined using a 2-D mathematical model of the SRM.

The torque waveform for optimal SRM made from steel 1010 is presented in Figure 2. The efficiency characteristic is presented in Figure 3.

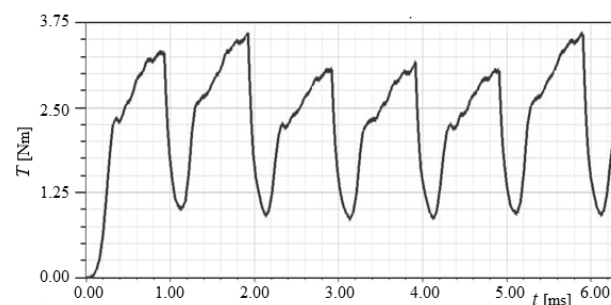


Fig.2. The torque waveform for motor with steel core

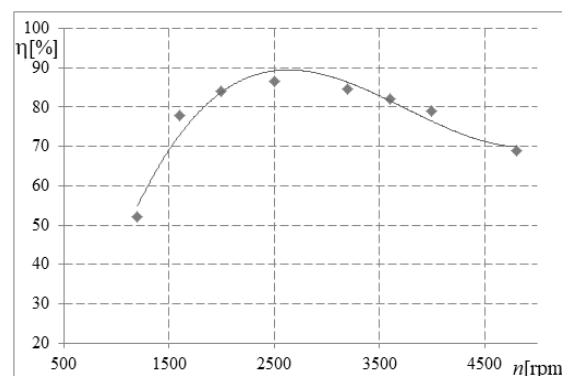


Fig.3. The efficiency characteristics of the SRM with steel core

The torque waveform for optimal SRM produced from M-19 laminated silicon steel is presented in Figure 4. The efficiency characteristics of the SRM with M-19 material are presented in Figure 5.

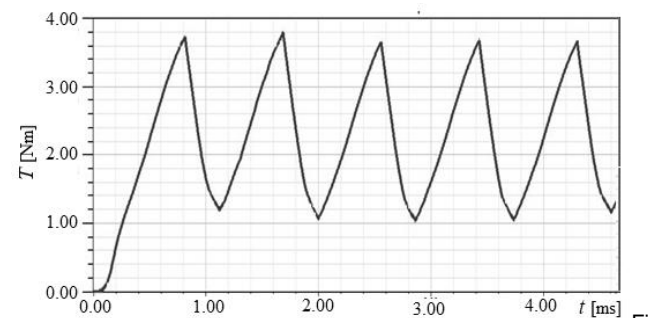


Fig.4. The torque waveform for SRM made from M-19

The optimal machine made of M-19 material has a lower efficiency value, but the motor maintains a similar efficiency through the wide range of velocity.

## Conclusions

The salp swarm algorithm was applied to constrained optimization of the SRM for electric vehicle applications. In the objective function, three functional parameters and one cost parameter were taken into account. The optimization calculations were made for two different materials used on core construction.

The obtained results of calculations show, that core construction made from steel 1010 allows to achieve higher efficiency values. Whereas, the higher average electromagnetic torque, lower torque ripple, and lower mass core material were obtained for optimal structure with M-19 material.

The presented results of calculations show, that the applied core material can have the impact of the final functional parameters of the optimized switched reluctance motor.

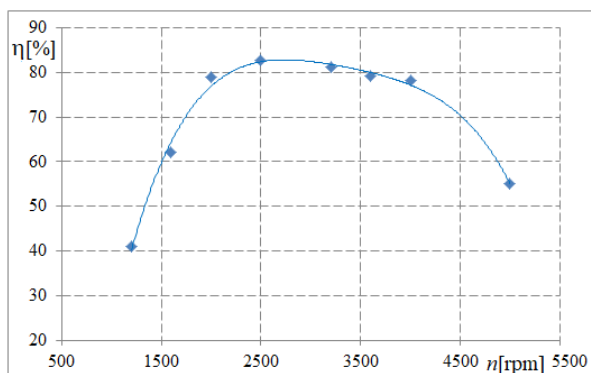


Fig.5. The efficiency characteristics of the SRM with laminated silicon steel

This research was funded by the Polish Government, grant number [0212/SBAD/0594].

**Authors:** Assistant professor Łukasz Knypiński, Poznan University of Technology, ul. Piotrowo 3a, 60-965 Poznan, Poland, e-mail: lukasz.knypiński@put.poznan.pl; Associate professor Bathina Venkateswararao, Siddhartha Engineering College, Vijayawada-520007, India; e-mail: bvrao.eee@gmail.com; Assistant professor Ramesh Devarapalli, Department of Electrical/ Electronics and Instrumentation Engineering, Institute of Chemical Technology, e-mail: Dr.R.Devarapalli@gmail.com; Professor Yvonnick Le Menach, Lille University of Technology, Lille, France, e-mail: yvonnick.le-menach@univ-lille.fr; Professor Mehmet Cunkas, Selcuk University, Konya, Turkey, mcunkas@selcuk.edu.tr.

## REFERENCES

- [1] Choi Y. K., Koh C. S., Pole-shape optimization of a switched-reluctance motor for torque ripple reduction, IEEE Trans. on Magnetics, vol. 43, no. 4, 1797-1800, 2007.
- [2] Xue X. D., Cheng K.W. E., Ng T. W., Cheung N.C., Multi-Objective Optimization Design of In-Wheel Switched Reluctance Motors in Electric Vehicles, IEEE Transaction on Industrial Electronics, vol.57, no.9, pp. 2980-2987, 2010.
- [3] Bilgin B., Emadi A., Krishnamurthy M., Design Considerations for Switched Reluctance Machines With a Higher Number of Rotor Poles, IEEE Transaction on Industrial Electronics, vol. 59, no. 10, pp.3745-3756, 2012.
- [4] Takeno M., Chiba A., Hoshi N., Ogasawara S., Takemoto M., Rahman M. A., Test Results and Torque Improvement of the 50kW Switched Reluctance Motor Designed for Hybrid Electric Vehicles, IEEE Transaction on Industry Applications, vol.48, no.4, pp. 1327-1334, 2012.
- [5] Kiyota K., Chiba A., Design of Switched Reluctance Motor Competitive to 60-kW IPMSM in Third-Generation Hybrid Electric Vehicle, IEEE Transaction on Industry Applications, vol. 48, no. 6, pp.2303-2309, 2012.
- [6] Kiyota K., Kakishima T., Chiba A., Comparison of Test Result and Design Stage Prediction of Switched Reluctance Motor Competitive With 60-kW Rare-Earth PM Motor, IEEE Transaction on Industrial Electronics, vol. 61, no. 10, pp. 5712-5721, pp.2564-2575, 2014.
- [7] Kakishima T., Kiyota K., Nakano S., Chiba A., Pole selection and vibration reduction of Switched Reluctance Motor for hybrid electric vehicles, 2014 IEEE Transportation Electrification Conference and Expo Asia-Pacific, Aug. 31-Sept. 3, 2014, pp. 1-4.
- [8] Ozawa I., Kosaka T., Matsui N., Less Rare-Earth Magnet-High Power Density Hybrid Excitation Motor Designed for Hybrid Electric Vehicle Drives, in Proceedings of the Eur. Conf. Power Electron. Appl, Barcelona, Spain, Sep. 8-10, 2009, pp. 1-10.
- [9] Wu S., Xu H., Zhang T., Gu Q., Wang B., Multi-Objective Optimization of an Axial Flux Permanent Magnet Brushless DC Motor with Arc-Shaped Magnets, Applied Sciences, vol. 12, no.11641, pp. 1-14, 2022.
- [10] Xue X. D., Cheng K. W. E., Ng T. W., Cheung N. C., Multi-Objective Optimization Design of In-Wheel Switched Reluctance Motors in Electric Vehicles, IEEE Transaction on Industrial Electronics, vol. 57, no. 9, pp. 2980-2987, 2010.
- [11] Minami S., Sanada M., Morimoto S., Inoue Y., Influence of ratio of external diameter to stack length on torque and efficiency in outer rotor SPMSMs, IEEE Energy Conversion Congress 2015, Montreal, pp. 1834-1839, 2015.
- [12] Huang R., A Hybrid Particle Swarm Optimization and Single-Objective Slap Swarm Optimization Algorithm Based MPPT Strategy, Journal of Physics: Conference Series, no. 2290, pp. 1-6, 2022.
- [13] Mirjalili S., Gandomi A. H., Zahra Mirjalili S., Saremi S., Faris H., Mohammad Mirjalili S., Salp Swarm Algorithm: A bio-inspired optimizer for engineering design problems, Advances in Eng. Software, pp. 1-29, 2017.
- [14] Knypiński Ł., Devarepalli R., Le Menach Y., Constrained optimization of the brushless DC motor using the salp swarm algorithm, Archives of Electrical Engineering, vol. 71, no. 3, pp. 775-787, 2022.
- [15] Khajezhadem M., Irajji A., Majdi A., Keawsawasvong S., Nehdi M. L., Adaptive Salp Swarm Algorithm for Optimization of Geotechnical Structures, Applied Sciences, vol. 12, no. 6749, pp. 1-23, 2022.
- [16] Andriushchenko E., Kallaste A., Hossain Mohammadi M., Lowther D. A., Heidar H., Sensitivity Analysis for Multi-Objective Optimization of Switched Reluctance Motors, Machines, vol. 10, no. 559, pp. 1-16, 2022.
- [17] Afifi M., Rezk H., Ibrahim M., El-Nemr M., Multi-Objective Optimization of Switched Reluctance Machine Design Using Jaya Algorithm (MO-Jaya), Mathematics, vol. 9, no. 1107, pp. 1-19, 2021.
- [18] Sun X., Wu J., Wang S., Diao K., Yang Z., Analysis of torque ripple and fault-tolerant capability for a 16/10 segmented switched reluctance motor in HEV applications, COMPEL, vol. 38, no. 6, pp. 1725-1737, 2019.
- [19] Knypiński Ł., Constrained optimization of line-start PM motor based on the gray wolf optimizer, Eksploatacja i Niezawodność – Maintenance and Reliability, vol. 23, no. 1, pp. 1-10, 2021.
- [20] Knypiński Ł., Kowalski K., Nowak L., Constrained optimization of the magnetostrictive actuator with the use of penalty function method, COMPEL, vol. 37, no. 5, pp. 1575-1584, 2018.
- [21] Oguntola B. M, Lorentzen R. J., Ensemble-based constrained optimization using an exterior penalty method, Journal of Petroleum Science and Engineering, vol. 207, no. 109165, 2021.
- [22] Knypiński Ł., A novel hybrid cuckoo search algorithm for optimization of a line-start PM synchronous motor, Bulletin of the Polish Academy of Sciences Technical Sciences, vol. 71, no. 1. pp. 1-8, 2023.